Preclinical evaluation of tumor microvascular response to a novel antiangiogenic/antitumor agent RO0281501 by dynamic contrast-enhanced MRI at 1.5 T

Manickam Muruganandham,[1] Mihaela Lupu,[1] Jonathan P. Dyke,[4] Cornelia Matei,[1] Michael Linn,[5] Kathryn Packman,[6] Kenneth Kolinsky,[6] Brian Higgins,[6] and Jason A. Koutcher[1,2,3]

Departments of [1]Medical Physics, [2]Radiology, and [3]Medicine, Memorial Sloan-Kettering Cancer Center; [4]Weill Cornell Medical College, Cornell University, New York, New York and Departments of [5]Non-Clinical Drug Safety and [6]Discovery Oncology, Hoffmann-La Roche, Inc., Nutley, New Jersey

Abstract

Inhibition of tumor angiogenesis is a promising approach in cancer treatment. The purpose of this study was to evaluate the vascular response of human lung tumor xenografts *in vivo* to RO0281501, an inhibitor of tyrosine kinase receptors, including vascular endothelial growth factor receptor 2, fibroblast growth factor receptor, and platelet-derived growth factor receptor, using dynamic contrast-enhanced magnetic resonance imaging (DCE-MRI). Human non–small cell lung carcinoma (H460a) xenografts grown s.c. in athymic *nu/nu* mice were treated p.o. with the antiangiogenic agent RO0281501. Treatment-induced changes in tumor volume, epiphyseal growth plate thickness, and microvessel density assessed by CD31 immunohistochemistry were analyzed. Tumor vascular permeability and perfusion were measured in tumors using DCE-MRI with gadopentetate dimeglumine on a 1.5 T clinical scanner to assess vascular function. Treatment with RO0281501 resulted in significant growth retardation of H460a tumors. RO0281501-treated tumors showed histologic evidence of growth plate thickening and relatively lower microvessel density compared with the controls. Regarding DCE-MRI variables, the initial slope of contrast uptake and Ak_{ep} were significantly decreased on day 7 of treatment. RO0281501 is a novel antiangiogenic/antitumor agent, which is active in the H460a xenograft model. Its effects on tumor vasculature can be monitored and assessed by DCE-MRI on a 1.5 T human MR scanner with clinically available gadopentetate dimeglumine contrast, which will facilitate clinical trials with this or similar agents. [Mol Cancer Ther 2006;5(8): 1950–7]

Introduction

Angiogenesis in solid tumors plays an important role in tumor growth, invasion, and metastasis by supplying nutrients and oxygen (1, 2). The concept of killing tumor cells by destroying tumor vasculature is gaining importance in cancer therapy (3). A variety of receptor tyrosine kinases, including vascular endothelial growth factor (VEGF) receptor (VEGFR), platelet-derived growth factor receptor, and fibroblast growth factor receptor, play important roles in promoting angiogenesis through transmission of proliferation and survival signals to endothelial cells in solid tumors (4). Hypoxia, a key attribute of solid tumors, leads to up-regulation of the most potent proangiogenic molecule VEGF (also known as vascular permeability factor) that is known to induce intracellular signaling in endothelial cells and act as a survival factor for both normal and tumor endothelium (5). Up-regulation of VEGF results in hyperpermeability of tumor vessels, permitting large plasma proteins to leak into the extravascular space. This in turn helps facilitate angiogenesis, continued tumor growth, and metastases (6, 7). Over the last several years, antiangiogenic therapy has moved from a conceptual idea through preclinical and clinical studies and is now found to be efficacious (8). Treatment with bevacizumab, a monoclonal antibody against VEGFR2, is effective as measured by different end points in the treatment in gastrointestinal tumors (9, 10), renal cell carcinomas (11), non–small cell lung cancer (12), and breast cancer (13).

Assessment of tumor angiogenesis and the effects of antiangiogenic treatments are most often carried out by histologic measures of microvessel density (MVD) and the soluble serum levels of angiogenesis factors (14). The reliability of the latter measure is subject to considerable dispute. Although measures of MVD provide a direct method of assessment, it is invasive as it requires tumor tissue specimens and provides only the morphologic information and not the functional status of vascular network. In addition, this approach does not allow repeated measurements on the same tumor during the course of treatment. Evaluation of treatment efficacy by

Received 1/6/06; revised 4/26/06; accepted 6/14/06.

Grant support: NIH grants 1R24CA83084-06, P50 CA86438, and P30 CA08748 and Hoffmann-La Roche, Inc. (Nutley, NJ).

The costs of publication of this article were defrayed in part by the payment of page charges. This article must therefore be hereby marked advertisement in accordance with 18 U.S.C. Section 1734 solely to indicate this fact.

Note: Part of this work was presented in AACR-National Cancer Institute-European Organization for Research and Treatment of Cancer International Conference on Molecular Targets and Cancer Therapeutics: Discovery, Biology, and Clinical Applications [poster B11]. Philadelphia (PA): 2005 Nov 14-18.

Requests for reprints: Jason A. Koutcher, Department of Medical Physics, Memorial Sloan-Kettering Cancer Center, 1275 York Avenue, New York, NY 10021. Phone: 212-639-8834; Fax: 212-717-3676. E-mail: koutchej@mskcc.org

doi:10.1158/1535-7163.MCT-06-0010

conventional measure of tumor size reduction using computed tomography or magnetic resonance imaging (MRI) may not be adequate because pure antiangiogenic treatments, which target host endothelial cells, are mainly expected to exert cytostatic effects, slowing or stopping tumor growth (15–17). Thus, information about functional status of tumor vessels will be important as the treatment-induced changes in tumor vascular physiology may occur well ahead of any objective reduction in tumor size. Dynamic contrast-enhanced MRI (DCE-MRI) is an imaging modality that allows for the uptake and clearance of contrast agents in tissues to be monitored over time. This can provide surrogate measures of tumor vascular function in response to antiangiogenic therapy (17–20) by permitting repeated measurements with a given tumor during the course of treatment. Although macromolecular contrast agents have been suggested to be suitable for the effective detection of antiangiogenic treatment-induced reduction in tumor vessel permeability (21), they are not presently available for clinical use. The clinically approved low molecular weight contrast agent gadopentetate dimeglumine (Gd-DTPA), however, has been used to investigate tumor vessel permeability both in preclinical (22–25) and clinical studies (26–29).

The primary goal of the present study was to evaluate the vascular response of H460a (human non–small cell lung carcinoma) xenografts in mouse to a novel antiangiogenic/antitumor agent RO0281501 by DCE-MRI on a 1.5 T clinical MRI scanner using Gd-DTPA contrast agent. RO0281501 is a novel pyrrolobenzodiazepine multitargeted kinase inhibitor (Fig. 1) that affects both proangiogenic tyrosine kinase receptors (VEGFR2, fibroblast growth factor receptor, and platelet-derived growth factor receptor) as well as tumor cell–related kinases culminating in dual antiangiogenic/cytotoxic mechanism of action (30, 31). Variables of contrast enhancement kinetics, the initial slope reflecting the perfusion status and a two-compartment model variable Ak_{ep} that relate to the vessel permeability, were derived to assess tumor vascular function and compared with the treatment-induced changes in tumor volume, epiphyseal growth plate thickness, and CD31-stained MVD.

Materials and Methods

Tumor Model and Drug Treatment

H460a cells (provided by Dr. Jack Roth, M. D. Anderson Cancer Center, Houston, TX) were grown in RPMI 1640 supplemented with 10% FCS. The cell concentrations for implant were 1×10^7 cells/0.2 mL suspended in HBSS with 20 mmol/L HEPES buffer and implanted s.c. in the right flank of female athymic *nu/nu* mice (National Cancer Institute-Frederick Cancer Research Center, Frederick, MD). Tumor volumes were calculated from the measures of three orthogonal diameters (d) as $(d_1 \times d_2 \times d_3) / 2$. Mice were randomized, and volume-matched tumors were selected for treatment and MRI studies. Initially, a spectrum of doses from 100 mg/kg b.i.d. down to 1.56 mg/kg b.i.d. (100, 50, 25, 12.5, 6.25, 3.125, and 1.56) was tested in H460a xenograft model in nude mice to optimize the dose and antitumor activity *in vivo*. Tumors with a volume of ~200 mm^3 (10–12 days after inoculation) were treated with antiangiogenic agent RO0281501 (6.25 mg/kg b.i.d. p.o.; $n = 14$) and equal volume of vehicle for RO0281501 ($n = 10$) daily for 14 days. The dose level of 6.25 mg/kg b.i.d. was selected as it was found to be optimal from our dose-finding study. Tumor volumes of treated groups were given as percentages of tumor volumes of the control groups (%T/C) using the following formula: $100 \times [(T - T_0) / (C - C_0)]$, where T represents mean tumor volume of a treated group on a specific day during the experiment, T_0 represents mean tumor volume of the same group on the first day of treatment, C represents mean tumor volume of a control group on a particular day of the experiment, and C_0 represents mean tumor volume of the same group on the first day of treatment. Tumor growth inhibition was calculated using the following formula: 100 − %T/C. The experimental procedures used for this study were reviewed and approved by the Institutional Animal Care and Use Committee.

Histology and Immunohistochemistry

Femurs from vehicle and RO0281501-treated mice were harvested after 14 days of treatment and fixed in formalin overnight. The specimens were then decalcified in formic acid HCl decalcification agent for 6 to 8 hours before processing them for paraffin embedding, sectioned, mounted on glass microscope slides, and stained with H&E for morphologic assessment of epiphyseal growth plate thickness.

For CD31 immunohistochemistry, three tumor samples each from vehicle and RO0281501-treated mice were harvested after 7 days of treatment and fixed in formalin overnight. Formalin-fixed tissues from the mice were trimmed, processed, embedded in paraffin, sectioned, and mounted on glass microscope slides. Immunohistochemical staining was done using the avidin-biotin immunoperoxidase technique. Unstained sections (5-μm thick) were deparaffinized and subjected to 10 minutes of heat-mediated epitope retrieval. Endogenous peroxidase was blocked by incubation with 3% H_2O_2 in methanol for 10 minutes, and nonspecific immunoglobulin binding was blocked by incubation with 10% rabbit serum in Ultra V blocking solution (Lab Vision Corp., Fremont, CA). The sections were incubated overnight at room temperature with primary antibody (anti-CD31/PECAM-specific M20: goat polyclonal antibody, Santa Cruz Biotechnology, Inc.,

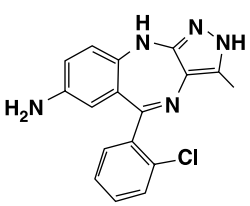

RO0281501

Figure 1. Structural formula of RO0281501.

Santa Cruz, CA) diluted in PBS (1:800). After rinsing with PBS, the sections were incubated in prediluted biotinylated rabbit anti-goat antibody (Biogenex, San Ramon, CA) for 1 hour at room temperature. After washes with PBS, the sections were incubated for 30 minutes with horseradish peroxidase–conjugated streptavidin (Lab Vision). Then, the sections were treated with Vector NovaRED chromogen (Vector Laboratories, Burlingame, CA) for 5 minutes. The slides were counterstained with Meyer's hematoxylin. MVD assessment was carried out as in Weidner et al. (2). Briefly, tumor sections were scanned at low magnification (×40) to identify the region of the section with the highest microvascular density (neovascular ''hotspot''), and then this area was counted at a magnification of ×200 for the microvasculature highlighted by the CD31 immunostaining. Tumor tissue sections from three vehicle and three RO0281501-treated mice were counted, and the mean was calculated for each treatment group. No statistical analysis was done due to small sample size (n = 3 per group).

DCE-MRI

A home-built small transmit-receive surface coil (1 cm diameter, single turn copper foil) covering only the tumor was used for imaging on a 1.5 T MRI scanner (Signa LX, General Electric, Milwaukee, WI). The mouse was restrained in the animal holder (60-mL syringe barrel with air holes), and a T2-weighted images in the transverse sections acquired using a fast spin-echo sequence with TR/TE of 4,000/85, echo train length of 12, field of view of 40 × 40 mm, matrix size of 256 × 128, slice thickness of 2 mm, four slices, no slice gap, and two excitations were used to select a single slice at the tumor center for the dynamic series. Dynamic images were acquired before and after injection of contrast agent using a fast spoiled gradient-echo sequence with TR/TE/θ of 9 ms/2 ms/30°, field of view of 40 × 40 mm, matrix size of 256 × 128, and slice thickness of 2 mm (yielding in-plane spatial resolution of 156 × 312 μm). A single slice at tumor center was acquired with 12 seconds of temporal resolution with two excitations and 64 time points in ~13 minutes. Injection of the contrast agent Gd-DTPA (0.2 mmol/kg; Magnevist, Berlex Laboratories, Wayne, NJ) as a bolus through a tail vein catheter was started at the onset of the fifth scan of the dynamic series. Imaging studies were conducted before the start of the therapy (baseline) and 24 hours and 7 days after the start of therapy.

DCE-MRI Data Analysis

Following on-line reconstruction, data were exported to a Sun Ultra 20 workstation (Sun Microsystems Inc., Palo Alto, CA) and analyzed using in-house software (32) written in Interactive Data Language version 6.0 (Research Systems, Inc., Boulder, CO.). Three different regions of interest consisting of whole tumor, tumor rim (1–2 mm band around tumor periphery), and tumor core were selected manually to investigate whether there was a difference in tumor response between the core and peripheral regions of the tumor. Time intensity curves were analyzed for each voxel in the image. The initial uptake slope was used for characterization of the response to the bolus. Calculation of the initial slope used a five-point sliding linear regression applied to the first 2 minutes of the time intensity curve. A baseline signal intensity value, SI_{pre}, was calculated as the mean intensity of three points before injection. The percentage increase per minute for each voxel was then calculated according to Eq. A.

$$\frac{\%SI}{\min} = \frac{Slope}{SI_{pre}} \cdot 100 \qquad \text{(A)}$$

In addition, a two-compartment model proposed by Hoffman et al. (33) based on that of Brix et al. (34), which incorporates rate constants of Gd-DTPA between the lesion to plasma compartments (k_{ep}) and elimination by the plasma (k_{el}), was used for the analysis. The plasma concentration was not directly measured because the clearance rate (k_{el}) can be estimated from the measured tissue curve. After a bolus injection (τ = bolus duration), if one assumes $k_{ep}\tau \ll 1$ and $k_{el}\tau \ll 1$, Hoffman's initial equation (33) reduces to Eq. B, which has three fitted variables: A (normalized amplitude), k_{ep} (min^{-1}), and k_{el} (min^{-1}).

$$\frac{S(t)}{S_0} \approx 1 + A\frac{k_{ep}(e^{-k_{ep}t} - e^{-k_{el}t})}{k_{el} - k_{ep}} \qquad \text{(B)}$$

The variables A and k_{ep}, which describe the contrast transfer between the lesion and plasma compartments, are fit independently. At short times after injection (small values of t), the right side of Eq. B reduces to $1 + Ak_{ep}t$; thus, the initial slope is proportional to Ak_{ep}.

Statistical Analysis

The changes in contrast kinetic variables and tumor volumes were analyzed using paired t test analysis. Statistical significance was assigned if $P < 0.05$.

Results

Antitumor Activity of RO0281501

RO0281501 treatment with doses <6.25 mg/kg b.i.d. was well tolerated with no noticeable body weight loss or overt toxicity compared with the vehicle group (data not shown). The mice treated with doses >6.25 mg/kg, unfortunately, exhibited higher mortality rate and gastrointestinal toxicity. Treatment with 6.25 mg/kg b.i.d. RO0281501 inhibited tumor growth by ~83% ($P < 0.001$) and 81% ($P < 0.0001$) compared with the vehicle-treated controls on 7 and 14 days after treatment, respectively (Fig. 2).

Immunohistochemical Evidence of Antiangiogenic Activity

The immunohistochemical staining for CD31 revealed ~43% reduction in mean MVD within tumors treated with RO0281501 compared with vehicle-treated controls (RO0281501 = 23 versus vehicle = 40.3; n = 3) after 7 days (Fig. 3A and B). Although statistical significance could not

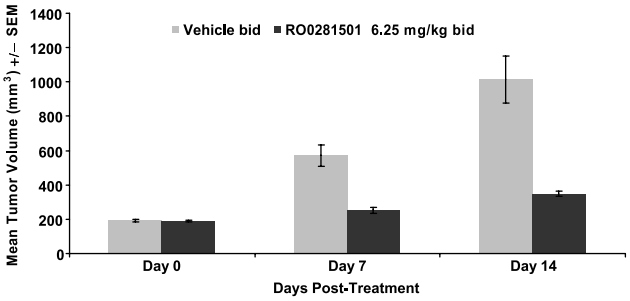

Figure 2. Mean tumor volume for tumors treated with vehicle and 6.25 mg/kg b.i.d. p.o. RO0281501. *Columns*, mean; *bars*, SE. Note the significant growth inhibition in the RO0281501-treated group.

be established due to small sample size, the trend is suggestive of RO0281501 targeting tumor vasculature. Agents targeting angiogenesis are known to cause retention of hypertrophic chondrocytes, resulting in epiphyseal growth plate thickening (35). When femurs from mice treated with RO0281501 were examined, histologic evidence of growth plate thickening was evident (Fig. 3D) compared with vehicle-treated mice (Fig. 3C) and suggests that RO0281501 indeed has antiangiogenic activity.

Pattern and Variables of DCE Kinetics in Tumors Treated with RO0281501

Contrast-enhanced images from the vehicle and RO0281501 group obtained before treatment, 24 hours, and 7 days after treatment are shown in Fig. 4. The tumor periphery exhibits a clear and strong signal enhancement, which was typical of almost all the tumors studied. Post-treatment changes in enhancement were different in control and RO0281501-treated tumors. The images obtained on day 7 after treatment depict visually appreciable reduction in the enhancement from the tumor rim region of RO0281501-treated tumor. The differences in tumor response between tumor periphery and core were investigated in the following section by selecting region of interests (ROI) from the respective regions for the analyses of contrast kinetic variables. Figure 5 shows contrast enhancement patterns observed in the periphery of a representative tumor (from both control and RO0281501 groups) before treatment and 24 hours and 7 days after treatment. A significantly different uptake and washout of contrast was observed in RO0281501-treated tumor (Fig. 5B) compared with the control (Fig. 5A) on day 7 after treatment. RO0281501-treated tumors showed a decrease in magnitude and rate of initial enhancement and a gradual increase in late phase of the contrast kinetics compared with the rapid washout observed in the control, reflecting the continuous trapping of contrast agent in tumors.

The effects of RO0281501 on H460a tumor vasculature as reflected by the contrast kinetic variables, slope of the initial enhancement and the model variable Ak_{ep} of tumors, are presented in Fig. 6. The pretreatment (baseline) slope and Ak_{ep} values of vehicle and RO0281501-treated animals showed no significant difference. On day 7, the tumor rim region of RO0281501-treated group showed a decrease of 55.4% ($P < 0.00007$) in the initial slope of contrast uptake (Fig. 6A) compared with the baseline. Similarly, 7 days after treatment, the reductions in Ak_{ep} (Fig. 6B) were most

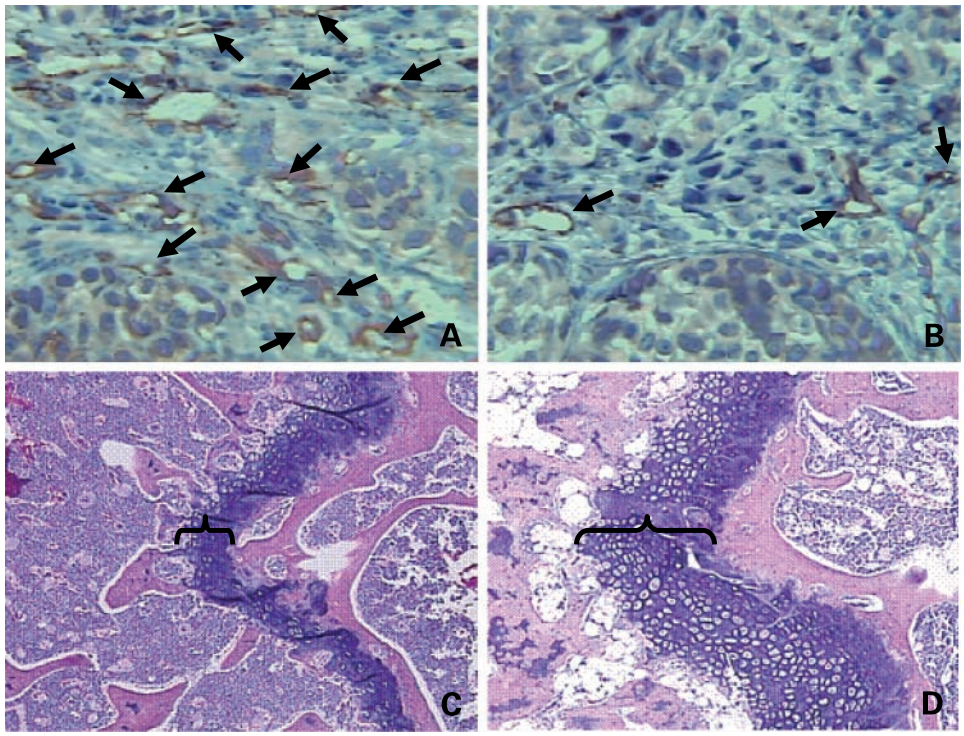

Figure 3. *Top,* representative CD31-stained H460a tumor sections from mice treated with vehicle (**A**) or 6.25 mg/kg b.i.d. RO0281501 (**B**) for 7 d. Formalin-fixed, paraffin-embedded tissue sections were stained with an anti-CD31 antibody to localize newly formed blood vessels (*arrows*). *Bottom,* representative H&E-stained femur sections from mice treated with vehicle (**C**) or 6.25 mg/kg b.i.d. RO0281501 (**D**) for 2 wks. Formalin-fixed, paraffin-embedded tissue sections were stained with H&E to examine epiphyseal growth plate thickness. Thickening of growth plate was clearly evident in mice treated with RO0281501 (**D**, *brackets*) compared with vehicle-treated mice (**C**).

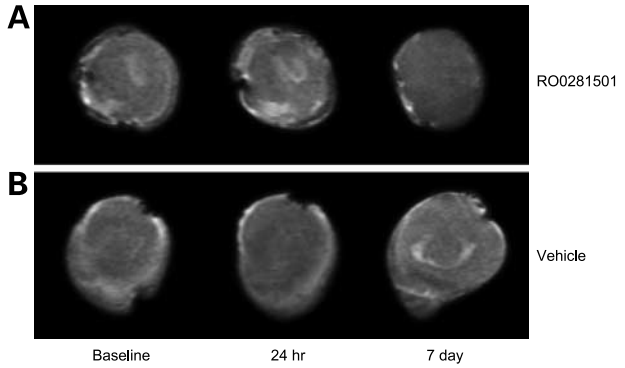

Figure 4. T1-weighted MR images from the DCE-MRI data set of a representative tumor corresponding to 5 min after contrast time point. **A**, control treated with vehicle for RO0281501 for 7 d. **B**, RO0281501-treated group (6.25 mg/kg b.i.d. p.o.) obtained before treatment (baseline) and 24 h and 7 d after treatment. DCE-MRI was done before treatment (baseline) and 24 h and 7 d after RO0281501 treatment. Only the tumor is seen in the image. Contrast enhancement kinetics were analyzed from the ROI consisting of the whole tumor, tumor rim, and tumor core.

significant in the rim of the tumor (50%; $P < 0.003$). The tumor core showed no significant change in slope (Fig. 6C) and Ak_{ep} (Fig. 6D) 7 days after treatment. The whole tumor analysis showed a 50.7% ($P < 0.005$) decrease in slope and 44.8% ($P < 0.04$) reduction in Ak_{ep} (Fig. 6E and F) 7 days after treatment. The magnitude of mean slope and Ak_{ep} values in the rim of tumors were almost twice that calculated for tumor core. This indicates that the periphery of the H460a tumors was highly vascularized/perfused as these portions of tumors are, in general, expected to have prominent angiogenic activity. The clear separations of the slope and Ak_{ep} values between baseline and day 7 after treatment observed from the tumor rim region well delineate the effects of treatment. At 24 hours after treatment, the slope and Ak_{ep} distributions are more scattered with all three ROIs (tumor rim, core, and the whole tumor). No significant differences were observed either in slope or Ak_{ep} values from all three ROIs with the controls.

Discussion

The results of this study show that a novel antiangiogenic compound, RO0281501, has both antitumor and vascular effects as shown in a human lung cancer model. The antiangiogenic effects can be monitored in early clinical trials by DCE-MRI using a 1.5 T human MR scanner with a clinically available contrast agent, Gd-DTPA. This may facilitate early response information for this agent. Preclinical studies, such as this one, may help select the optimal time for clinical studies to evaluate drug activity in patients being treated with these agents.

In addition to MVD measurements, we also used DCE-MRI to evaluate response. Assessment of the therapeutic efficacy of novel kinase inhibitors in individual patients during drug development can be challenging because response is often manifested by disease stabilization and not tumor shrinkage (16, 17). Thus, our results do not show tumor shrinkage but decreases in tumor growth rate. Although this effect is readily discernible in preclinical trials, in the clinic, slowing of disease growth is hard to evaluate during the study and only can be seen at the end of the trial based on comparison with control cohorts. Thus, DCE-MRI may be a valuable adjunct in the evaluation of antiangiogenic drugs. Using DCE-MRI, it has been reported that different antiangiogenic agents may result in different tumor vascular responses. In xenografts of glioblastoma multiforme, anti-VEGF antibodies were reported to affect both vessel permeability and fractional plasma volume (36). In contrast, an inhibitor of VEGFR2 kinase activity, PTK787/ZK222584, has been shown to alter only the tumor vessel permeability without significant changes in fractional plasma volume in experimental breast tumors (37). Although choice of contrast agent, small or macromolecular, has also been suggested to influence the reliability of response assessment in antiangiogenic treatments (21), a recent study at 1.5 T using the small molecular agent Gd-DTPA has clearly shown reliable measures of tumor microvascular permeability and a correlation with MVD measurements in a human colon carcinoma model (25). In addition, recent investigations have shown reproducible DCE-MRI measurements of vascular permeability using Gd-DTPA in patients with solid tumors (38).

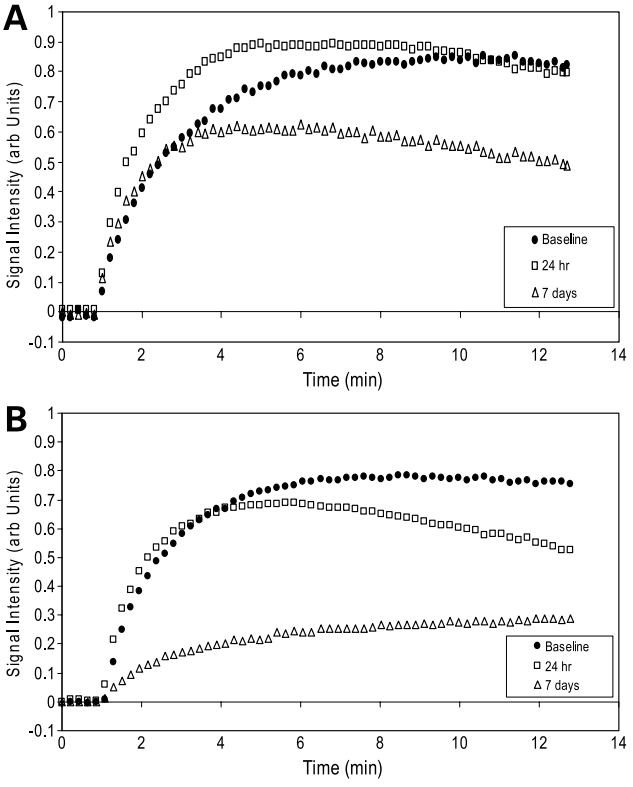

Figure 5. Patterns of contrast enhancement kinetics in the tumor rim region of a representative tumor treated with vehicle for RO0281501 (**A**) and RO0281501 (**B**). Note the differences in uptake and washout of the contrast on day 7 between the RO0281501-treated and control group.

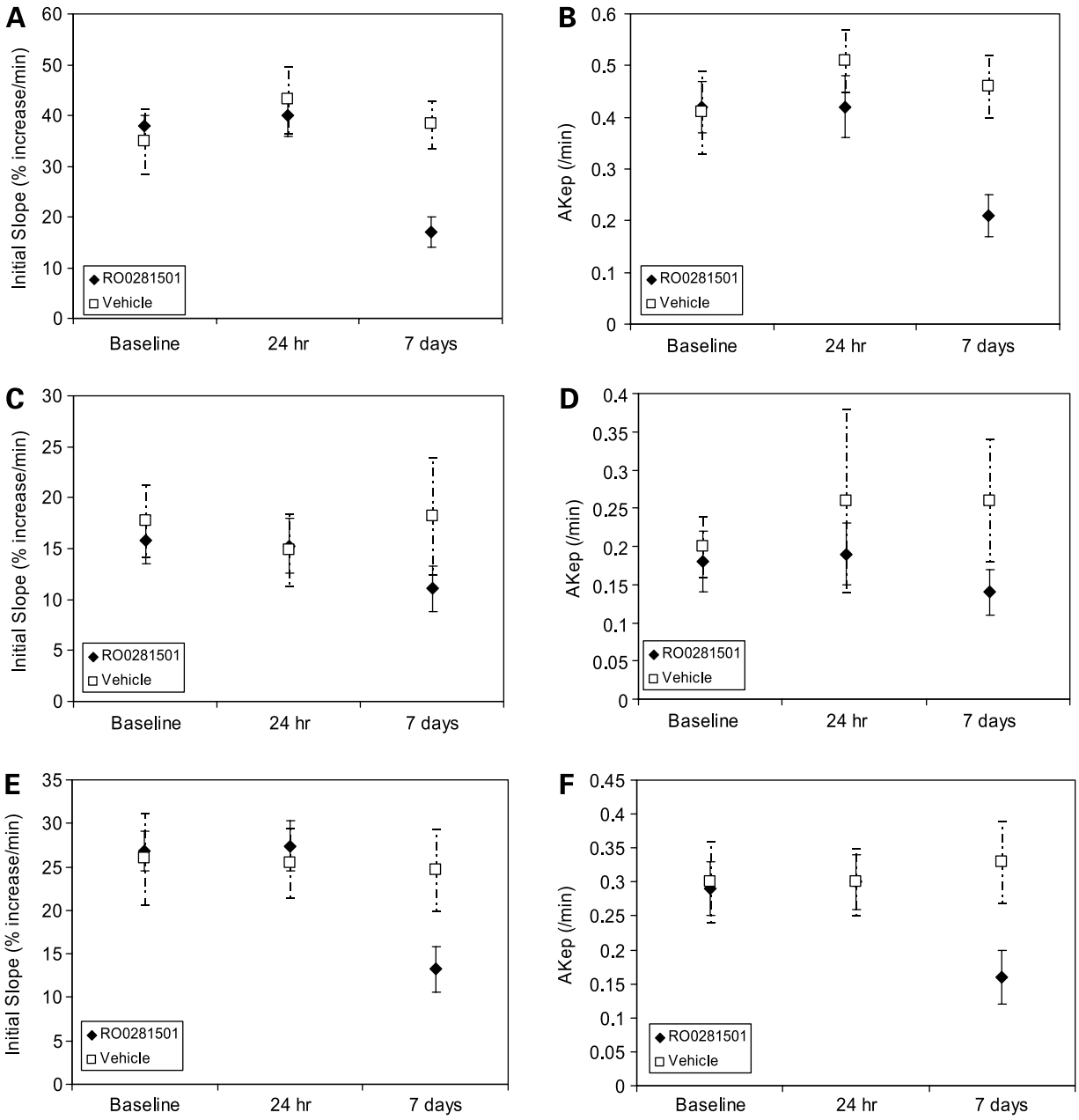

Figure 6. Effects of RO0281501 on tumor vasculature. Contrast kinetic variables, the initial slope of contrast uptake and the two-compartment model variable Ak_{ep}, among individual tumors in both control (n = 10) and RO0281501-treated group (n = 14). *Points,* mean; *bars,* SE. **A** and **B,** tumor rim ROI slope and Ak_{ep}. **C** and **D,** tumor core ROI slope and Ak_{ep}. **E** and **F,** whole tumor ROI slope and Ak_{ep}. Note that the slope and Ak_{ep} values from the regions of both tumor rim (**A** and **B**) and whole tumor (**E** and **F**) were significantly reduced on 7 d after treatment with RO0281501 compared with the baseline. The tumor core showed no significant change in slope (**C**) and Ak_{ep} (**D**) 7 d after RO0281501 treatment.

In the present study, tumor vascular function was assessed using an estimate of initial slope of the contrast agent uptake and the compartment model variable Ak_{ep}. In theory, the constant A should depend only on the precontrast T1 of the tissues and be proportional to extravascular extracellular space; however, in practice it may depend on perfusion. Similarly, the variable k_{ep} is assumed to be more sensitive to vessel leakiness than A, although again in practice its dependence of vascular volume and extracellular volume may limit its sensitivity. Thus, both permeability and perfusion, the variables of microcirculation suitable for characterizing the status of tumor vascularization that contribute to Ak_{ep} and thus are expected to decrease during process of vascular normalization or pruning hypothesized from antiangiogenic treatments (39), have been measured and shown to change

post-RO0281501 as expected. Reduction in tumor perfusion, vessel permeability, or combination of both after 7 days of RO0281501 treatment likely induced the observed decrease in slope and Ak_{ep} in both tumor rim and whole tumor ROIs (Fig. 6A, B, E, and F). However, the measurements at 24 hours showed no significant change in these vascular variables and exhibit more scattered distribution. These findings agree with the significant inhibition of tumor growth observed after 7 days of treatment. Absence of any reduction in tumor size coupled with very slow tumor progression observed during the entire course of treatment clearly reveals that RO0281501 induces growth-inhibitory effects. The reduced MVD in the RO0281501-treated tumors compared with vehicle-treated controls confirms the inhibition of angiogenesis.

DCE-MRI analysis of the mean of all voxels from the whole tumor often may not be optimal for the evaluation of antiangiogenic efficacy because highly enhancing well-vascularized regions of tumor could respond differently than regions of necrosis. Comparison of results in the present study from three different ROIs reveals the minimal effects in the core region of the H460a tumors. Significant antivascular effects were observed both in the whole tumor region (50.7% and 44.8% reduction in slope and Ak_{ep}, respectively) and in the tumor periphery (55.4% and 50% decrease in slope and Ak_{ep}, respectively). Although we expected large differences in magnitude of the effects between the whole tumor and tumor rim regions, the observed differences were only modest in the present study. This could be due to the criteria we set for selection of tumor rim ROI [i.e., ~2-mm band around the periphery instead of selecting only the highly enhancing regions (so-called ''hotspots'') from the tumor periphery]. We plan to investigate these aspects in detail in future studies. The differences in the degree of responses observed between different tumor regions will be important for the dose-finding studies as the magnitude of expected vascular effects may be dose dependent. They also have significant implications for therapy trials because it might be therapeutically beneficial to combine this drug with radiation, which would be more effective on the more vascular rim region of the tumor.

Previous DCE-MRI studies assessing the efficacy of antiangiogenic agents in preclinical tumor models mainly used macromolecular contrast agents (40). Only a few recent studies have used low molecular contrast agents. Gossmann et al. (36) measured a very significant reduction in vascular permeability of intracranial tumors in rats as a result of an anti-VEGF antibody treatment. Another study on testing the efficacy of chronic treatment of KDR/Flt-1 inhibitor, PTK787/ZK222584, in murine renal tumor model reported ~50% decrease in vascular permeability (41). More recently, Checkley et al. (24) investigated the acute effects of a VEGFR2 tyrosine kinase inhibitor, ZD6474, for a range of doses using Gd-DTPA contrast agent and reported dose-related reductions in vascular permeability. In addition to finding the optimum effective dose of these agents, the selection of the time of DCE-MRI assessment is also important. In the present study, the protracted (14 days) treatment of RO0281501 resulted in a significant reduction in slope of the initial contrast uptake and Ak_{ep} by day 7. DCE-MRI measurements at 24 hours after treatment did not show any significant change. In addition, our pilot experiments involving DCE-MRI measurements on day 3 of RO0281501 treatment (data not shown) failed to show any modifications in vascular status. These results confirm the observations made by others that time course studies are crucial in evaluating the efficacy of antiangiogenic agents (42) as different agents may have different time-dependent effects. Incorporation of time course measurements in preclinical testing could help to carefully plan patient treatment and examination schedules in early-stage clinical trials. RO0281501 is a novel agent that inhibits tyrosine kinase receptors (VEGFR2, fibroblast growth factor receptor, and platelet-derived growth factor receptor) involved in angiogenesis. Our present results will be useful in planning and evaluation of early-stage clinical testing of this compound in tumor types amenable to this imaging modality.

References

1. Folkman J. The role of angiogenesis in tumor growth. Semin Cancer Biol 1992;3:65 – 71.
2. Weidner N, Semple JP, Welch WR, Folkman J. Tumor angiogenesis and metastasis—correlation in invasive breast carcinoma. N Engl J Med 1991; 324:1 – 8.
3. Tozer GM, Bicknell R. Therapeutic targeting of the tumor vasculature. Semin Radiat Oncol 2004;14:222 – 32.
4. Papetti M, Herman IM. Mechanisms of normal and tumor-derived angiogenesis. Am J Physiol Cell Physiol 2002;282:C947 – 70.
5. Acker T, Plate KH. Role of hypoxia in tumor angiogenesis—molecular and cellular angiogenic crosstalk. Cell Tissue Res 2003;314:145 – 55.
6. Dvorak HF, Brown LF, Detmar M, Dvorak AM. Vascular permeability factor/vascular endothelial growth factor, microvascular hyperpermeability, and angiogenesis. Am J Pathol 1995;146:1029 – 39.
7. Zetter BR. Angiogenesis and tumor metastasis. Annu Rev Med 1998; 49:407 – 24.
8. Kim DW, Lu B, Hallahan DE. Receptor tyrosine kinase inhibitors as anti-angiogenic agents. Curr Opin Investig Drugs 2004;5:597 – 604.
9. Kabbinavar F, Hurwitz HI, Fehrenbacher L, et al. Phase II, randomized trial comparing bevacizumab plus fluorouracil (FU)/leucovorin (LV) with FU/LV alone in patients with meastatic colorectal cancer. J Clin Oncol 2003;21:60 – 5.
10. Kindler HL, Friberg G, Singh DA, et al. Phase II trial of bevacizumab plus gemcitabine in patients with advanced pancreatic cancer. J Clin Oncol 2005;23:8033 – 40.
11. Yang JC, Haworth L, Sherry RM, et al. A randomized trial of bevacizumab, an anti-vascular endothelial growth factor antibody, for metastatic renal cancer. N Engl J Med 2003;349:427 – 34.
12. Johnson DH, Fehrenbacher L, Novotny WF, et al. Randomized phase II trial comparing bevacizumab plus carboplatin and paclitaxel with carboplatin and paclitaxel alone in previously untreated locally advanced or metastatic non-small-cell lung cancer. J Clin Oncol 2004;22:2184 – 91.
13. Wedam SB, Low JA, Yang SX, et al. Antiangiogenic and antitumor effects of bevacizumab in patients with inflammatory and locally advanced breast cancer. J Clin Oncol 2006;24:769 – 77.
14. Davis DW, McConkey DJ, Abbruzzese JL, Herbst RS. Surrogate markers in antiangiogenesis clinical trials. Br J Cancer 2003;89:8 – 14.
15. O'Reilly MS, Holmgren L, Chen C, Folkman J. Angiostatin induces and sustains dormancy of human primary tumors in mice. Nat Med 1996;2: 689 – 92.
16. Korn EL, Arbuck SG, Pluda JM, Simon R, Kaplan RS, Christian MC.

Clinical trial designs for cytostatic agents: are new approaches needed? J Clin Oncol 2001;19:265 – 72.

17. Morgan B, Horsfield MA, Steward WP. The role of imaging in the clinical development of antiangiogenic agents. Hematol Oncol Clin North Am 2004;18:1183 – 206.

18. Choyke PL, Dwyer AJ, Knopp MV. Functional tumor imaging with dynamic contrast-enhanced magnetic resonance imaging. J Magn Reson Imaging 2003;17:509 – 20.

19. Neeman M, Dafni H. Structural, functional, and molecular MR imaging of the microvasculature. Annu Rev Biomed Eng 2003;5:29 – 56.

20. Padhani AR. MRI for assessing antivascular cancer treatments. Br J Radiol 2003;76:S60 – 80.

21. Turetschek K, Preda A, Novikov V, et al. Tumor microvascular changes in antiangiogenic treatment: assessment by magnetic resonance contrast media of different molecular weights. J Magn Reson Imaging 2004;20:138 – 44.

22. Furman-Haran E, Margalit R, Grobgeld D, Degani H. Dynamic contrast-enhanced magnetic resonance imaging reveals stress-induced angiogenesis in MCF7 human breast tumors. Proc Natl Acad Sci U S A 1996;93:6247 – 51.

23. Checkley D, Tessier JJ, Wedge SR, et al. Dynamic contrast-enhanced MRI of vascular changes induced by the VEGF-signalling inhibitor ZD4190 in human tumour xenografts. Magn Reson Imaging 2003;21:475 – 82.

24. Checkley D, Tessier JJ, Kendrew J, Waterton JC, Wedge SR. Use of dynamic contrast-enhanced MRI to evaluate acute treatment with ZD6474, a VEGF signalling inhibitor, in PC-3 prostate tumours. Br J Cancer 2003;89:1889 – 95.

25. de Lussanet QG, Langereis S, Beets-Tan RG, et al. Dynamic contrast-enhanced MR imaging kinetic parameters and molecular weight of dendritic contrast agents in tumor angiogenesis in mice. Radiology 2005;235:65 – 72.

26. Tofts PS, Berkowitz B, Schnall MD. Quantitative analysis of dynamic Gd-DTPA enhancement in breast tumors using a permeability model. Magn Reson Med 1995;33:564 – 8.

27. Su MY, Cheung YC, Fruehauf JP, et al. Correlation of dynamic contrast enhancement MRI parameters with microvessel density and VEGF for assessment of angiogenesis in breast cancer. J Magn Reson Imaging 2003;18:467 – 77.

28. Morgan B, Thomas AL, Drevs J, et al. Dynamic contrast-enhanced magnetic resonance imaging as a biomarker for the pharmacological response of PTK787/ZK 222584, an inhibitor of the vascular endothelial growth factor receptor tyrosine kinases, in patients with advanced colorectal cancer and liver metastases: results from two phase I studies. J Clin Oncol 2003;21:3955 – 64.

29. Padhani AR, Dzik-Jurasz A. Perfusion MR imaging of extracranial tumor angiogenesis. Top Magn Reson Imaging 2004;15:41 – 57.

30. Higgins B, Kolinsky K, Yang H, et al. Pharmacokinetics, antitumor and antiangiogenic activity of the novel dual acting mitosis and angiogenesis inhibitor RO0281501 (MAI). Proc AACR-NCI-EORTC international conference on molecular targets and cancer therapeutics: discovery, biology, and clinical applications [poster B210]. Philadelphia (PA): 2005 Nov 14-18.

31. Higgins B, Kolinsky K, Nevins T, et al. *In vivo* activity of the novel dual acting mitotic and angiogenesis inhibitor RO0281501 (MAI) in the rat corneal pocket and rat syngeneic tumor models [poster B217]. Proc AACR-NCI-EORTC international conference on molecular targets and cancer therapeutics: discovery, biology, and clinical applications [poster B11]. Philadelphia (PA): 2005 Nov 14-18.

32. Dyke JP, Panicek DM, Healey JH, et al. Osteogenic and Ewing sarcomas: estimation of necrotic fraction during induction chemotherapy with dynamic contrast-enhanced MR imaging. Radiology 2003;228: 271 – 8.

33. Hoffmann U, Brix G, Knopp MV, Hess T, Lorenz WJ. Pharmacokinetic mapping of the breast: a new method for dynamic MR mammography. Magn Reson Med 1995;33:506 – 14.

34. Brix G, Semmler W, Port R, Schad LR, Layer G, Lorenz WJ. Pharmacokinetic parameters in CNS Gd-DTPA enhanced MR imaging. J Comput Assist Tomogr 1991;15:621 – 8.

35. Hall AP, Westwood FR, Wadsworth PF. Review of the effects of anti-angiogenic compounds on the epiphyseal growth plate. Toxicol Pathol 2006;34:131 – 47.

36. Gossmann A, Helbich TH, Kuriyama N, et al. Dynamic contrast-enhanced magnetic resonance imaging as a surrogate marker of tumor response to anti-angiogenic therapy in a xenograft model of glioblastoma multiforme. J Magn Reson Imaging 2002;15:233 – 40.

37. Turetschek K, Preda A, Floyd E, et al. MRI monitoring of tumor response following angiogenesis inhibition in an experimental human breast cancer model. Eur J Nucl Med Mol Imaging 2003;30:448 – 55.

38. Jackson A, Jayson GC, Li KL, et al. Reproducibility of quantitative dynamic contrast-enhanced MRI in newly presenting glioma. Br J Radiol 2003;76:153 – 62.

39. Tong RT, Boucher Y, Kozin SV, Winkler F, Hicklin DJ, Jain RK. Vascular normalization by vascular endothelial growth factor receptor 2 blockade induces a pressure gradient across the vasculature and improves drug penetration in tumors. Cancer Res 2004;64:3731 – 6.

40. Padhani AR. MRI for assessing antivascular cancer treatments. Br J Radiol 2003;76 Spec No 1:S60 – 80.

41. Drevs J, Muller-Driver R, Wittig C, et al. PTK787/ZK 222584, a specific vascular endothelial growth factor-receptor tyrosine kinase inhibitor, affects the arnatomy of the tumor vascular bed and the functional vascular properties as detected by dynamic enhanced magnetic resonance imaging. Cancer Res 2002;62:4015 – 22.

42. Marzola P, Degrassi A, Calderan L, et al. *In vivo* assessment of antiangiogenic activity of SU6668 in an experimental colon carcinoma model. Clin Cancer Res 2004;10:739 – 50.

Molecular Cancer Therapeutics

Preclinical evaluation of tumor microvascular response to a novel antiangiogenic/antitumor agent RO0281501 by dynamic contrast-enhanced MRI at 1.5 T

Manickam Muruganandham, Mihaela Lupu, Jonathan P. Dyke, et al.

Mol Cancer Ther 2006;5:1950-1957.